

Measurement of $B^0\text{-}\bar{B}^0$ Flavor Oscillations in Hadronic B^0 Decays

B. Aubert,¹ D. Boutigny,¹ J.-M. Gaillard,¹ A. Hicheur,¹ Y. Karyotakis,¹ J. P. Lees,¹ P. Robbe,¹ V. Tisserand,¹
A. Palano,² A. Pompili,² G. P. Chen,³ J. C. Chen,³ N. D. Qi,³ G. Rong,³ P. Wang,³ Y. S. Zhu,³ G. Eigen,⁴
B. Stugu,⁴ G. S. Abrams,⁵ A. W. Borgland,⁵ A. B. Breon,⁵ D. N. Brown,⁵ J. Button-Shafer,⁵ R. N. Cahn,⁵
A. R. Clark,⁵ M. S. Gill,⁵ A. V. Gritsan,⁵ Y. Groysman,⁵ R. G. Jacobsen,⁵ R. W. Kadel,⁵ J. Kadyk,⁵ L. T. Kerth,⁵
Yu. G. Kolomensky,⁵ J. F. Kral,⁵ C. LeClerc,⁵ M. E. Levi,⁵ G. Lynch,⁵ P. J. Oddone,⁵ M. Pripstein,⁵ N. A. Roe,⁵
A. Romosan,⁵ M. T. Ronan,⁵ V. G. Shelkov,⁵ A. V. Telnov,⁵ W. A. Wenzel,⁵ T. J. Harrison,⁶ C. M. Hawkes,⁶
D. J. Knowles,⁶ S. W. O'Neale,⁶ R. C. Penny,⁶ A. T. Watson,⁶ N. K. Watson,⁶ T. Deppermann,⁷ K. Goetzen,⁷
H. Koch,⁷ M. Kunze,⁷ B. Lewandowski,⁷ K. Peters,⁷ H. Schmuecker,⁷ M. Steinke,⁷ N. R. Barlow,⁸ W. Bhimji,⁸
N. Chevalier,⁸ P. J. Clark,⁸ W. N. Cottingham,⁸ B. Foster,⁸ C. Mackay,⁸ F. F. Wilson,⁸ K. Abe,⁹ C. Hearty,⁹
T. S. Mattison,⁹ J. A. McKenna,⁹ D. Thiessen,⁹ S. Jolly,¹⁰ A. K. McKemey,¹⁰ V. E. Blinov,¹¹ A. D. Bukin,¹¹
D. A. Bukin,¹¹ A. R. Buzykaev,¹¹ V. B. Golubev,¹¹ V. N. Ivanchenko,¹¹ A. A. Korol,¹¹ E. A. Kravchenko,¹¹
A. P. Onuchin,¹¹ S. I. Serednyakov,¹¹ Yu. I. Skovpen,¹¹ V. I. Telnov,¹¹ A. N. Yushkov,¹¹ D. Best,¹² M. Chao,¹²
D. Kirkby,¹² A. J. Lankford,¹² M. Mandelkern,¹² S. McMahon,¹² D. P. Stoker,¹² K. Arisaka,¹³ C. Buchanan,¹³
S. Chun,¹³ D. B. MacFarlane,¹⁴ S. Prell,¹⁴ Sh. Rahatlou,¹⁴ G. Raven,¹⁴ V. Sharma,¹⁴ C. Campagnari,¹⁵
B. Dahmes,¹⁵ P. A. Hart,¹⁵ N. Kuznetsova,¹⁵ S. L. Levy,¹⁵ O. Long,¹⁵ A. Lu,¹⁵ J. D. Richman,¹⁵ W. Verkerke,¹⁵
J. Beringer,¹⁶ A. M. Eisner,¹⁶ M. Grothe,¹⁶ C. A. Heusch,¹⁶ W. S. Lockman,¹⁶ T. Pulliam,¹⁶ T. Schalk,¹⁶
R. E. Schmitz,¹⁶ B. A. Schumm,¹⁶ A. Seiden,¹⁶ M. Turri,¹⁶ W. Walkowiak,¹⁶ D. C. Williams,¹⁶ M. G. Wilson,¹⁶
E. Chen,¹⁷ G. P. Dubois-Felsmann,¹⁷ A. Dvoretzki,¹⁷ D. G. Hitlin,¹⁷ S. Metzler,¹⁷ J. Oyang,¹⁷ F. C. Porter,¹⁷
A. Ryd,¹⁷ A. Samuel,¹⁷ M. Weaver,¹⁷ S. Yang,¹⁷ R. Y. Zhu,¹⁷ S. Devmal,¹⁸ T. L. Geld,¹⁸ S. Jayatilleke,¹⁸
G. Mancinelli,¹⁸ B. T. Meadows,¹⁸ M. D. Sokoloff,¹⁸ T. Barillari,¹⁹ P. Bloom,¹⁹ M. O. Dima,¹⁹ W. T. Ford,¹⁹
U. Nauenberg,¹⁹ A. Olivas,¹⁹ P. Rankin,¹⁹ J. Roy,¹⁹ J. G. Smith,¹⁹ W. C. van Hoek,¹⁹ J. Blouw,²⁰ J. L. Harton,²⁰
M. Krishnamurthy,²⁰ A. Soffer,²⁰ W. H. Toki,²⁰ R. J. Wilson,²⁰ J. Zhang,²⁰ T. Brandt,²¹ J. Brose,²¹
T. Colberg,²¹ M. Dickopp,²¹ R. S. Dubitzky,²¹ A. Hauke,²¹ E. Maly,²¹ R. Müller-Pfefferkorn,²¹ S. Otto,²¹
K. R. Schubert,²¹ R. Schwierz,²¹ B. Spaan,²¹ L. Wilden,²¹ D. Bernard,²² G. R. Bonneaud,²² F. Brochard,²²
J. Cohen-Tanugi,²² S. Ferrag,²² S. T'Jampens,²² Ch. Thiebaux,²² G. Vasileiadis,²² M. Verderi,²² A. Anjomshoaa,²³
R. Bernet,²³ A. Khan,²³ D. Lavin,²³ F. Muheim,²³ S. Playfer,²³ J. E. Swain,²³ J. Tinslay,²³ M. Falbo,²⁴
C. Borean,²⁵ C. Bozzi,²⁵ S. Dittongo,²⁵ L. Piemontese,²⁵ E. Treadwell,²⁶ F. Anulli,²⁷ * R. Baldini-Ferrolì,²⁷
A. Calcaterra,²⁷ R. de Sangro,²⁷ D. Falciari,²⁷ G. Finocchiaro,²⁷ P. Patteri,²⁷ I. M. Peruzzi,²⁷ * M. Piccolo,²⁷
Y. Xie,²⁷ A. Zallo,²⁷ S. Bagnasco,²⁸ A. Buzzo,²⁸ R. Contri,²⁸ G. Crosetti,²⁸ M. Lo Vetere,²⁸ M. Macri,²⁸
M. R. Monge,²⁸ S. Passaggio,²⁸ F. C. Pastore,²⁸ C. Patrignani,²⁸ M. G. Pia,²⁸ E. Robutti,²⁸ A. Santroni,²⁸
S. Tosi,²⁸ M. Morii,²⁹ R. Bartoldus,³⁰ R. Hamilton,³⁰ U. Mallik,³⁰ J. Cochran,³¹ H. B. Crawley,³¹ P.-A. Fischer,³¹
J. Lamsa,³¹ W. T. Meyer,³¹ E. I. Rosenberg,³¹ G. Grosdidier,³² C. Hast,³² A. Höcker,³² H. M. Lacker,³²
S. Laplace,³² V. Lepeltier,³² A. M. Lutz,³² S. Plaszczynski,³² M. H. Schune,³² S. Trincaz-Duvold,³² G. Wormser,³²
R. M. Bionta,³³ V. Brigljević,³³ D. J. Lange,³³ M. Mugge,³³ K. van Bibber,³³ D. M. Wright,³³ A. J. Bevan,³⁴
J. R. Fry,³⁴ E. Gabathuler,³⁴ R. Gamet,³⁴ M. George,³⁴ M. Kay,³⁴ D. J. Payne,³⁴ R. J. Sloane,³⁴ C. Touramanis,³⁴
M. L. Aspinwall,³⁵ D. A. Bowerman,³⁵ P. D. Dauncey,³⁵ U. Egede,³⁵ I. Eschrich,³⁵ N. J. W. Gunawardane,³⁵
J. A. Nash,³⁵ P. Sanders,³⁵ D. Smith,³⁵ D. E. Azzopardi,³⁶ J. J. Back,³⁶ G. Bellodi,³⁶ P. Dixon,³⁶ P. F. Harrison,³⁶
R. J. L. Potter,³⁶ H. W. Shorthouse,³⁶ P. Strother,³⁶ P. B. Vidal,³⁶ G. Cowan,³⁷ S. George,³⁷ M. G. Green,³⁷
A. Kurup,³⁷ C. E. Marker,³⁷ P. McGrath,³⁷ T. R. McMahon,³⁷ S. Ricciardi,³⁷ F. Salvatore,³⁷ G. Vaitsas,³⁷
D. Brown,³⁸ C. L. Davis,³⁸ J. Allison,³⁹ R. J. Barlow,³⁹ J. T. Boyd,³⁹ A. C. Forti,³⁹ J. Fullwood,³⁹ F. Jackson,³⁹
G. D. Lafferty,³⁹ N. Savvas,³⁹ J. H. Weatherall,³⁹ J. C. Williams,³⁹ A. Farbin,⁴⁰ A. Jawahery,⁴⁰ V. Lillard,⁴⁰
J. Olsen,⁴⁰ D. A. Roberts,⁴⁰ J. R. Schieck,⁴⁰ G. Blaylock,⁴¹ C. Dallapiccola,⁴¹ K. T. Flood,⁴¹ S. S. Hertzbach,⁴¹
R. Kofler,⁴¹ V. B. Koptchev,⁴¹ T. B. Moore,⁴¹ H. Staengle,⁴¹ S. Willocq,⁴¹ B. Brau,⁴² R. Cowan,⁴² G. Sciolla,⁴²
F. Taylor,⁴² R. K. Yamamoto,⁴² M. Milek,⁴³ P. M. Patel,⁴³ F. Palombo,⁴⁴ J. M. Bauer,⁴⁵ L. Cremaldi,⁴⁵
V. Eschenburg,⁴⁵ R. Kroeger,⁴⁵ J. Reidy,⁴⁵ D. A. Sanders,⁴⁵ D. J. Summers,⁴⁵ J. Y. Nief,⁴⁶ P. Taras,⁴⁶

H. Nicholson,⁴⁷ C. Cartaro,⁴⁸ N. Cavallo,⁴⁸,† G. De Nardo,⁴⁸ F. Fabozzi,⁴⁸ C. Gatto,⁴⁸ L. Lista,⁴⁸ P. Paolucci,⁴⁸
 D. Piccolo,⁴⁸ C. Sciacca,⁴⁸ J. M. LoSecco,⁴⁹ J. R. G. Alsmiller,⁵⁰ T. A. Gabriel,⁵⁰ J. Brau,⁵¹ R. Frey,⁵¹
 E. Grauges,⁵¹ M. Iwasaki,⁵¹ N. B. Sinev,⁵¹ D. Strom,⁵¹ F. Colecchia,⁵² F. Dal Corso,⁵² A. Dorigo,⁵² F. Galeazzi,⁵²
 M. Margoni,⁵² G. Michelon,⁵² M. Morandin,⁵² M. Posocco,⁵² M. Rotondo,⁵² F. Simonetto,⁵² R. Stroili,⁵²
 E. Torassa,⁵² C. Voci,⁵² M. Benayoun,⁵³ H. Briand,⁵³ J. Chauveau,⁵³ P. David,⁵³ Ch. de la Vaissière,⁵³ L. Del
 Buono,⁵³ O. Hamon,⁵³ F. Le Diberder,⁵³ Ph. Leruste,⁵³ J. Ocariz,⁵³ L. Roos,⁵³ J. Stark,⁵³ P. F. Manfredi,⁵⁴
 V. Re,⁵⁴ V. Speziali,⁵⁴ E. D. Frank,⁵⁵ L. Gladney,⁵⁵ Q. H. Guo,⁵⁵ J. Panetta,⁵⁵ C. Angelini,⁵⁶ G. Batignani,⁵⁶
 S. Bettarini,⁵⁶ M. Bondioli,⁵⁶ F. Bucci,⁵⁶ E. Campagna,⁵⁶ M. Carpinelli,⁵⁶ F. Forti,⁵⁶ M. A. Giorgi,⁵⁶ A. Lusiani,⁵⁶
 G. Marchiori,⁵⁶ F. Martinez-Vidal,⁵⁶ M. Morganti,⁵⁶ N. Neri,⁵⁶ E. Paoloni,⁵⁶ M. Rama,⁵⁶ G. Rizzo,⁵⁶ F. Sandrelli,⁵⁶
 G. Simi,⁵⁶ G. Triggiani,⁵⁶ J. Walsh,⁵⁶ M. Haire,⁵⁷ D. Judd,⁵⁷ K. Paick,⁵⁷ L. Turnbull,⁵⁷ D. E. Wagoner,⁵⁷
 J. Albert,⁵⁸ P. Elmer,⁵⁸ C. Lu,⁵⁸ V. Miftakov,⁵⁸ S. F. Schaffner,⁵⁸ A. J. S. Smith,⁵⁸ A. Tumanov,⁵⁸ E. W. Varnes,⁵⁸
 G. Cavoto,⁵⁹ D. del Re,⁵⁹ R. Faccini,^{14,59} F. Ferrarotto,⁵⁹ F. Ferroni,⁵⁹ E. Lamanna,⁵⁹ M. A. Mazzoni,⁵⁹
 S. Morganti,⁵⁹ G. Piredda,⁵⁹ F. Safai Tehrani,⁵⁹ M. Serra,⁵⁹ C. Voena,⁵⁹ S. Christ,⁶⁰ R. Waldi,⁶⁰ T. Adye,⁶¹
 N. De Groot,⁶¹ B. Franek,⁶¹ N. I. Geddes,⁶¹ G. P. Gopal,⁶¹ S. M. Xella,⁶¹ R. Aleksan,⁶² S. Emery,⁶²
 A. Gaidot,⁶² S. F. Ganzhur,⁶² P.-F. Giraud,⁶² G. Hamel de Monchenault,⁶² W. Kozanecki,⁶² M. Langer,⁶²
 G. W. London,⁶² B. Mayer,⁶² B. Serfass,⁶² G. Vasseur,⁶² Ch. Yèche,⁶² M. Zito,⁶² M. V. Purohit,⁶³ H. Singh,⁶³
 A. W. Weidemann,⁶³ F. X. Yumiceva,⁶³ I. Adam,⁶⁴ D. Aston,⁶⁴ N. Berger,⁶⁴ A. M. Boyarski,⁶⁴ G. Calderini,⁶⁴
 M. R. Convery,⁶⁴ D. P. Coupal,⁶⁴ D. Dong,⁶⁴ J. Dorfan,⁶⁴ W. Dunwoodie,⁶⁴ R. C. Field,⁶⁴ T. Glanzman,⁶⁴
 S. J. Gowdy,⁶⁴ T. Haas,⁶⁴ T. Himel,⁶⁴ T. Hryn'ova,⁶⁴ M. E. Huffer,⁶⁴ W. R. Innes,⁶⁴ C. P. Jessop,⁶⁴
 M. H. Kelsey,⁶⁴ P. Kim,⁶⁴ M. L. Kocian,⁶⁴ U. Langenegger,⁶⁴ D. W. G. S. Leith,⁶⁴ S. Luitz,⁶⁴ V. Luth,⁶⁴
 H. L. Lynch,⁶⁴ H. Marsiske,⁶⁴ S. Menke,⁶⁴ R. Messner,⁶⁴ D. R. Muller,⁶⁴ C. P. O'Grady,⁶⁴ V. E. Ozcan,⁶⁴
 A. Perazzo,⁶⁴ M. Perl,⁶⁴ S. Petrak,⁶⁴ H. Quinn,⁶⁴ B. N. Ratcliff,⁶⁴ S. H. Robertson,⁶⁴ A. Roodman,⁶⁴
 A. A. Salnikov,⁶⁴ T. Schietinger,⁶⁴ R. H. Schindler,⁶⁴ J. Schwiening,⁶⁴ A. Snyder,⁶⁴ A. Soha,⁶⁴ S. M. Spanier,⁶⁴
 J. Stelzer,⁶⁴ D. Su,⁶⁴ M. K. Sullivan,⁶⁴ H. A. Tanaka,⁶⁴ J. Va'vra,⁶⁴ S. R. Wagner,⁶⁴ A. J. R. Weinstein,⁶⁴
 W. J. Wisniewski,⁶⁴ D. H. Wright,⁶⁴ C. C. Young,⁶⁴ P. R. Burchat,⁶⁵ C. H. Cheng,⁶⁵ T. I. Meyer,⁶⁵ C. Roat,⁶⁵
 R. Henderson,⁶⁶ W. Bugg,⁶⁷ H. Cohn,⁶⁷ J. M. Izen,⁶⁸ I. Kitayama,⁶⁸ X. C. Lou,⁶⁸ F. Bianchi,⁶⁹ M. Bona,⁶⁹
 D. Gamba,⁶⁹ L. Bosisio,⁷⁰ G. Della Ricca,⁷⁰ L. Lanceri,⁷⁰ P. Poropat,⁷⁰ G. Vuagnin,⁷⁰ R. S. Panvini,⁷¹
 C. M. Brown,⁷² P. D. Jackson,⁷² R. Kowalewski,⁷² J. M. Roney,⁷² H. R. Band,⁷³ E. Charles,⁷³ S. Dasu,⁷³
 A. M. Eichenbaum,⁷³ H. Hu,⁷³ J. R. Johnson,⁷³ R. Liu,⁷³ F. Di Lodovico,⁷³ Y. Pan,⁷³ R. Prepost,⁷³ I. J. Scott,⁷³
 S. J. Sekula,⁷³ J. H. von Wimmersperg-Toeller,⁷³ S. L. Wu,⁷³ Z. Yu,⁷³ T. M. B. Kordich,⁷⁴ and H. Neal⁷⁴

(The BABAR Collaboration)

¹Laboratoire de Physique des Particules, F-74941 Annecy-le-Vieux, France

²Università di Bari, Dipartimento di Fisica and INFN, I-70126 Bari, Italy

³Institute of High Energy Physics, Beijing 100039, China

⁴University of Bergen, Inst. of Physics, N-5007 Bergen, Norway

⁵Lawrence Berkeley National Laboratory and University of California, Berkeley, CA 94720, USA

⁶University of Birmingham, Birmingham, B15 2TT, United Kingdom

⁷Ruhr Universität Bochum, Institut für Experimentalphysik 1, D-44780 Bochum, Germany

⁸University of Bristol, Bristol BS8 1TL, United Kingdom

⁹University of British Columbia, Vancouver, BC, Canada V6T 1Z1

¹⁰Brunel University, Uxbridge, Middlesex UB8 3PH, United Kingdom

¹¹Budker Institute of Nuclear Physics, Novosibirsk 630090, Russia

¹²University of California at Irvine, Irvine, CA 92697, USA

¹³University of California at Los Angeles, Los Angeles, CA 90024, USA

¹⁴University of California at San Diego, La Jolla, CA 92093, USA

¹⁵University of California at Santa Barbara, Santa Barbara, CA 93106, USA

¹⁶University of California at Santa Cruz, Institute for Particle Physics, Santa Cruz, CA 95064, USA

¹⁷California Institute of Technology, Pasadena, CA 91125, USA

¹⁸University of Cincinnati, Cincinnati, OH 45221, USA

¹⁹University of Colorado, Boulder, CO 80309, USA

²⁰Colorado State University, Fort Collins, CO 80523, USA

²¹Technische Universität Dresden, Institut für Kern- und Teilchenphysik, D-01062 Dresden, Germany

²²Ecole Polytechnique, F-91128 Palaiseau, France

²³University of Edinburgh, Edinburgh EH9 3JZ, United Kingdom

²⁴Elon University, Elon University, NC 27244-2010, USA

²⁵Università di Ferrara, Dipartimento di Fisica and INFN, I-44100 Ferrara, Italy

- ²⁶Florida A&M University, Tallahassee, FL 32307, USA
²⁷Laboratori Nazionali di Frascati dell'INFN, I-00044 Frascati, Italy
²⁸Università di Genova, Dipartimento di Fisica and INFN, I-16146 Genova, Italy
²⁹Harvard University, Cambridge, MA 02138, USA
³⁰University of Iowa, Iowa City, IA 52242, USA
³¹Iowa State University, Ames, IA 50011-3160, USA
³²Laboratoire de l'Accélérateur Linéaire, F-91898 Orsay, France
³³Lawrence Livermore National Laboratory, Livermore, CA 94550, USA
³⁴University of Liverpool, Liverpool L69 3BX, United Kingdom
³⁵University of London, Imperial College, London, SW7 2BW, United Kingdom
³⁶Queen Mary, University of London, E1 4NS, United Kingdom
³⁷University of London, Royal Holloway and Bedford New College, Egham, Surrey TW20 0EX, United Kingdom
³⁸University of Louisville, Louisville, KY 40292, USA
³⁹University of Manchester, Manchester M13 9PL, United Kingdom
⁴⁰University of Maryland, College Park, MD 20742, USA
⁴¹University of Massachusetts, Amherst, MA 01003, USA
⁴²Massachusetts Institute of Technology, Laboratory for Nuclear Science, Cambridge, MA 02139, USA
⁴³McGill University, Montréal, QC, Canada H3A 2T8
⁴⁴Università di Milano, Dipartimento di Fisica and INFN, I-20133 Milano, Italy
⁴⁵University of Mississippi, University, MS 38677, USA
⁴⁶Université de Montréal, Laboratoire René J. A. Lévesque, Montréal, QC, Canada H3C 3J7
⁴⁷Mount Holyoke College, South Hadley, MA 01075, USA
⁴⁸Università di Napoli Federico II, Dipartimento di Scienze Fisiche and INFN, I-80126, Napoli, Italy
⁴⁹University of Notre Dame, Notre Dame, IN 46556, USA
⁵⁰Oak Ridge National Laboratory, Oak Ridge, TN 37831, USA
⁵¹University of Oregon, Eugene, OR 97403, USA
⁵²Università di Padova, Dipartimento di Fisica and INFN, I-35131 Padova, Italy
⁵³Universités Paris VI et VII, Lab de Physique Nucléaire H. E., F-75252 Paris, France
⁵⁴Università di Pavia, Dipartimento di Elettronica and INFN, I-27100 Pavia, Italy
⁵⁵University of Pennsylvania, Philadelphia, PA 19104, USA
⁵⁶Università di Pisa, Scuola Normale Superiore and INFN, I-56010 Pisa, Italy
⁵⁷Prairie View A&M University, Prairie View, TX 77446, USA
⁵⁸Princeton University, Princeton, NJ 08544, USA
⁵⁹Università di Roma La Sapienza, Dipartimento di Fisica and INFN, I-00185 Roma, Italy
⁶⁰Universität Rostock, D-18051 Rostock, Germany
⁶¹Rutherford Appleton Laboratory, Chilton, Didcot, Oxon, OX11 0QX, United Kingdom
⁶²DAPNIA, Commissariat à l'Energie Atomique/Saclay, F-91191 Gif-sur-Yvette, France
⁶³University of South Carolina, Columbia, SC 29208, USA
⁶⁴Stanford Linear Accelerator Center, Stanford, CA 94309, USA
⁶⁵Stanford University, Stanford, CA 94305-4060, USA
⁶⁶TRIUMF, Vancouver, BC, Canada V6T 2A3
⁶⁷University of Tennessee, Knoxville, TN 37996, USA
⁶⁸University of Texas at Dallas, Richardson, TX 75083, USA
⁶⁹Università di Torino, Dipartimento di Fisica Sperimentale and INFN, I-10125 Torino, Italy
⁷⁰Università di Trieste, Dipartimento di Fisica and INFN, I-34127 Trieste, Italy
⁷¹Vanderbilt University, Nashville, TN 37235, USA
⁷²University of Victoria, Victoria, BC, Canada V8W 3P6
⁷³University of Wisconsin, Madison, WI 53706, USA
⁷⁴Yale University, New Haven, CT 06511, USA

(Dated: December 31, 2001)

Flavor oscillations of neutral B mesons have been studied in e^+e^- annihilation data collected with the BABAR detector at center-of-mass energies near the $\Upsilon(4S)$ resonance. The data sample used for this purpose consists of events in which one B^0 meson is reconstructed in a hadronic decay mode, while the flavor of the recoiling B^0 is determined with a tagging algorithm that exploits the correlation between the flavor of the heavy quark and the charges of its decay products. From the time development of the observed mixed and unmixed final states we determine the B^0 - \bar{B}^0 oscillation frequency Δm_d to be $0.516 \pm 0.016(stat) \pm 0.010(syst)$ ps⁻¹.

PACS numbers: 12.15.Hh, 11.30.Er, 13.25.Hw

In the Standard Model, B^0 - \bar{B}^0 mixing [1] occurs through second-order weak diagrams involving the ex-

change of up-type quarks, with the top quark contributing the dominant amplitude. A measurement of the mass

difference Δm_d between the mass eigenstates is therefore sensitive to the value of the Cabibbo-Kobayashi-Maskawa [2] matrix element V_{td} . The phenomenon of particle-anti-particle mixing in the neutral B meson system was first seen almost fifteen years ago [3]. The oscillation frequency Δm_d has been measured with both time-integrated and time-dependent techniques [4].

In this Letter we present a measurement of time-dependent mixing based on a sample of 32 million $B\bar{B}$ pairs recorded at the $\Upsilon(4S)$ resonance with the BABAR detector at the Stanford Linear Accelerator Center. This study and a related CP asymmetry measurement [5] are described in more detail in Ref. [6]. At the PEP-II asymmetric-energy e^+e^- collider, the $\Upsilon(4S)$ provides a source of $B^0\bar{B}^0$ pairs moving along the e^- beam direction (z axis) with a known Lorentz boost of $\beta\gamma = 0.55$, allowing a novel technique for determining Δm_d .

The $B^0\text{-}\bar{B}^0$ mixing probability, for a given B^0 lifetime τ , is a function of Δm_d and the proper decay-time difference Δt between the two neutral B mesons produced in a coherent P -wave state in the $\Upsilon(4S)$ event. The result is a time-dependent probability to observe *unmixed* (+), $B^0\bar{B}^0$, or *mixed* (−), B^0B^0 and $\bar{B}^0\bar{B}^0$, events:

$$\text{Prob}(B^0\bar{B}^0 \rightarrow B^0\bar{B}^0, B^0B^0 \text{ or } \bar{B}^0\bar{B}^0) \propto e^{-|\Delta t|/\tau} (1 \pm \cos \Delta m_d \Delta t). \quad (1)$$

The effect can be measured by reconstructing one B in a flavor eigenstate, referred to as B_{rec} , while the remaining charged particles originating from the decay of the other B , referred to as B_{tag} , are used to identify, or “tag”, its flavor as a B^0 or \bar{B}^0 . The charges of identified leptons and kaons are the primary indicators, although other information in the event can also be used to identify the flavor of B_{tag} . The time difference $\Delta t = t_{\text{rec}} - t_{\text{tag}} \simeq \Delta z / \beta\gamma c$ is determined from the separation Δz of the decay vertices for the flavor-eigenstate and tagging B decays along the boost direction. The tagging and vertexing algorithms used in this analysis are nearly identical to those employed for CP violation studies, in which one B is fully reconstructed in a CP eigenstate [5].

The value of Δm_d is extracted from a tagged flavor-eigenstate B^0 sample with a simultaneous unbinned maximum likelihood fit to the Δt distributions of mixed and unmixed events. There are two principal experimental factors that complicate the probability distribution given by Eq. (1). First, the tagging algorithm, which classifies events into categories i depending on the source of the available tagging information, incorrectly identifies the flavor of B_{tag} with a probability w_i . This mistag rate reduces the observed amplitude of the oscillation by a factor $(1 - 2w_i)$. Second, the resolution for Δt is comparable to the oscillation period and must be well understood. The probability density functions (PDFs) for the unmixed and mixed signal events, $\mathcal{H}_{\pm, \text{sig}}$, can be expressed as the convolution of the underlying Δt distribu-

tion for the i^{th} tagging category,

$$h_{\pm}(\Delta t; \Delta m_d, w_i) = \frac{e^{-|\Delta t|/\tau}}{4\tau} [1 \pm (1 - 2w_i) \cos \Delta m_d \Delta t],$$

with a Δt resolution function containing parameters \hat{a}_j . A log-likelihood function is then constructed by summing $\ln \mathcal{H}_{\pm, \text{sig}}$ over all events within each of the tagging categories. The likelihood is maximized to extract simultaneously the mistag rates w_i , the resolution function parameters \hat{a}_j , and the mixing parameter Δm_d .

The BABAR detector is described in detail elsewhere [7]. Charged particles are detected and their momenta measured by a combination of a 40-layer drift chamber (DCH) and a five-layer silicon vertex tracker (SVT) embedded in a 1.5-T solenoidal magnetic field. B_{rec} decay vertices are reconstructed with a resolution of typically $65 \mu\text{m}$ along the boost direction. A detector of internally reflected Cherenkov radiation (DIRC) is used for charged hadron identification. Kaons are identified with a neural network based on the likelihood ratios in the SVT and DCH, derived from dE/dx measurements, and in the DIRC, calculated by comparing the observed and expected pattern of Cherenkov light for either kaons or pions. A finely segmented CsI(Tl) electromagnetic calorimeter (EMC) is used to detect photons and neutral hadrons, and to identify electrons. Electron candidates are required to have a ratio of EMC energy to track momentum, an EMC cluster shape, DCH dE/dx , and DIRC Cherenkov angle consistent with expectation. The instrumented flux return (IFR) is segmented and contains resistive plate chambers for muon and neutral hadron identification. Muon candidates are required to have IFR hits located along the extrapolated DCH track, an IFR penetration length, and an energy deposit in the EMC consistent with the muon hypothesis.

Neutral B mesons are reconstructed in a sample of multihadron events in the flavor eigenstate decay modes $D^{(*)-}\pi^+$, $D^{(*)-}\rho^+$, $D^{(*)-}a_1^+$ and $J/\psi K^{*0}$. The decay channels $K^+\pi^-$, $K^+\pi^-\pi^0$, $K^+\pi^+\pi^-\pi^-$ and $K_s^0\pi^+\pi^-$ are used to reconstruct \bar{D}^0 candidates, while the modes $K^+\pi^-\pi^-$ and $K_s^0\pi^-$ are used for D^- candidates. Charged D^{*-} candidates are formed by combining a \bar{D}^0 with a soft π^- . Finally, the B^0 candidates are formed by combining a D^{*-} or D^- candidate with a π^+ , ρ^+ ($\rho^+ \rightarrow \pi^+\pi^0$) or a_1^+ ($a_1^+ \rightarrow \pi^+\pi^-\pi^+$); likewise, $B^0 \rightarrow J/\psi K^{*0}$ candidates are reconstructed from combinations of J/ψ candidates, in the decay modes e^+e^- and $\mu^+\mu^-$, with a K^{*0} ($K^{*0} \rightarrow K^+\pi^-$). The selection and reconstruction of these decay chains and the selection of multihadron events, including continuum suppression, is described in more detail in Ref. [8].

Neutral B candidates are identified by the difference ΔE between the energy of the candidate and the beam energy $\sqrt{s}/2$ in the center-of-mass frame, and the beam-energy substituted mass m_{ES} , calculated from $\sqrt{s}/2$ and

the reconstructed momentum of the B candidate. Candidates are selected by requiring $m_{\text{ES}} > 5.2 \text{ GeV}/c^2$ and ΔE within ± 2.5 standard deviations of 0 (typically $|\Delta E| < 40 \text{ MeV}$). When multiple candidates in a given event are selected (with probability of about 0.25%), only the one with the smallest $|\Delta E|$ is retained.

After the daughter tracks of the B_{rec} are removed, the remaining tracks are analyzed to determine the flavor of the B_{tag} . For this purpose, we use the flavor tagging information carried by primary leptons from semileptonic B decays, charged kaons, soft pions from D^* decays, and high momentum charged particles, to assign an event to a single tagging category.

Events are assigned a **Lepton** tag if they contain an identified lepton with a center-of-mass momentum greater than 1.0 or 1.1 GeV/c for electrons and muons, respectively. The momentum requirement selects mostly primary leptons by suppressing opposite-sign leptons from semileptonic charm decays. If the sum of charges of all identified kaons is non-zero, the event is assigned a **Kaon** tag. The final two tags involve a multivariable analysis based on a neural network, which is trained to identify primary leptons, kaons, and soft pions, and the momentum and charge of the track with the maximum center-of-mass momentum. Depending on the output of the neural net, events are assigned either an NT1 (more certain) tag, an NT2 (less certain) tag, or are not tagged at all (about 30% of all events) and excluded from the analysis.

Tagging assignments are made mutually exclusive by the hierarchical use of the tags. Events with a **Lepton** tag and no conflicting **Kaon** tag are assigned to the **Lepton** category. If no **Lepton** tag exists, but the event has a **Kaon** tag, it is assigned to the **Kaon** category. Otherwise events with neural network tags are assigned to corresponding neural network categories.

The decay time difference Δt between B decays is determined from the measured separation $\Delta z = z_{\text{rec}} - z_{\text{tag}}$ along the z axis between the reconstructed $B_{\text{rec}}(z_{\text{rec}})$ and flavor-tagging decay $B_{\text{tag}}(z_{\text{tag}})$ vertex. This measured Δz is converted into Δt with the use of the known $\Upsilon(4S)$ boost, including a correction on an event-by-event basis for the direction of the B mesons with respect to the z direction in the $\Upsilon(4S)$ frame. The Δt resolution is dominated by the z resolution of the tag vertex position. Reconstruction of the B_{tag} decay vertex starts with all tracks in the event except those incorporated in B_{rec} . In order to reduce the contamination from D meson decay products, those identified as kaons are also excluded. An additional constraint is provided by the calculated B_{tag} production point and three-momentum, determined from the momentum of the B_{rec} candidate, its decay vertex, the average position of the interaction point, and the $\Upsilon(4S)$ boost. Tracks with a large contribution to the χ^2 are iteratively removed from the fit until those remaining (≥ 1) have a reasonable fit probability or all tracks

are removed. Only events with a reconstructed B_{tag} vertex, $|\Delta t| < 20 \text{ ps}$ and $\sigma_{\Delta t} < 1.4 \text{ ps}$ are retained (about 84%), where $\sigma_{\Delta t}$ is the measurement error derived from the vertex fits.

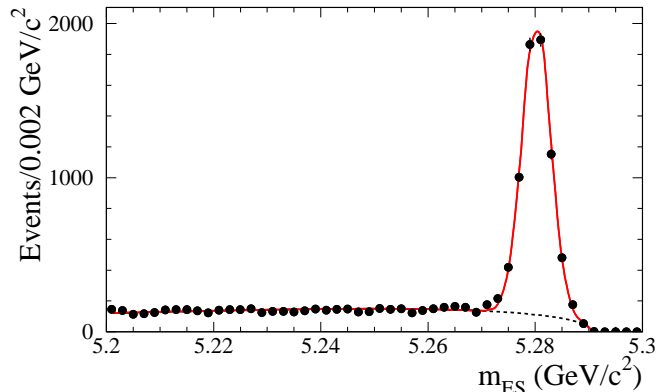


FIG. 1: Distribution of m_{ES} for all B^0 candidates with a flavor tag and a reconstructed tag vertex.

The distribution of m_{ES} for the selected candidates is shown in Fig. 1, where the result of a fit with a Gaussian distribution for the signal and an ARGUS function [9] for the background is also displayed. The fitted number of signal events and their purity (for $m_{\text{ES}} > 5.27 \text{ GeV}/c^2$) are 6347 ± 89 and $(85.8 \pm 0.5)\%$, respectively. The sample composition by tagging category is given in Table I.

TABLE I: Signal yields per tagging category, obtained from the m_{ES} distributions after all selection requirements. The purity is quoted for $m_{\text{ES}} > 5.27 \text{ GeV}/c^2$.

Category	Tagged	Purity (%)
Lepton	1097 ± 34	96.0 ± 0.7
Kaon	3156 ± 63	84.6 ± 0.7
NT1	798 ± 31	88.9 ± 1.2
NT2	1293 ± 43	79.4 ± 1.3

In the likelihood fit, the Δt resolution function is approximated by a sum of three Gaussian distributions (core, tail, and outlier) with different means and widths,

$$\mathcal{R}(\delta_t; \hat{a}) = \sum_{k=1}^2 \frac{f_k}{S_k \sigma_{\Delta t} \sqrt{2\pi}} \exp\left(-\frac{(\delta_t - b_k \sigma_{\Delta t})^2}{2(S_k \sigma_{\Delta t})^2}\right) + \frac{f_3}{\sigma_3 \sqrt{2\pi}} \exp\left(-\frac{\delta_t^2}{2\sigma_3^2}\right),$$

where $\delta_t = \Delta t - \Delta t_{\text{true}}$. The sum of the fractions f_k is constrained to unity. For the core and tail Gaussians, the widths $\sigma_k = S_k \times \sigma_{\Delta t}$ are the event-by-event measurement errors scaled by a common factor S_k . The scale factor of the tail Gaussian is fixed to the Monte Carlo value since it is strongly correlated with the other resolution function parameters. The third Gaussian, with

a fixed width of $\sigma_3 = 8$ ps, accounts for outlier events with incorrectly reconstructed vertices (less than 1% of events). A separate core bias coefficient $b_{1,i}$ is allowed for each tagging category i to account for small shifts due to inclusion of charm decay products in the tag vertex, while a common bias coefficient b_2 is used for the tail component. These offsets are proportional to $\sigma_{\Delta t}$ since both the size of the bias and the resolution for z_{tag} depend kinematically on the polar angle of the flight direction of the charm daughter. The tail and outlier fractions and the scale factors are assumed to be the same for all decay modes, since the z_{tag} measurement dominates the resolution for Δt . This assumption is confirmed by Monte Carlo studies. Separate resolution parameters are used for two different data-reconstruction periods, referred to as **Run1** and **Run2**, which mainly differ in vertex performance and tracking efficiency.

In the presence of backgrounds, additional terms must be added to the signal PDF $\mathcal{H}_{\pm,\text{sig}}$ for each background source,

$$\mathcal{H}_{\pm,i} = f_{i,\text{sig}}\mathcal{H}_{\pm,\text{sig}} + \sum_{j=\text{bkgd}} f_{i,j}\mathcal{B}_{\pm,i,j}(\Delta t; \hat{b}_{\pm,i,j}),$$

where the background PDFs $\mathcal{B}_{\pm,i,j}$ provide an empirical description for the Δt distribution of the background events in each tagging category i of the sample. The fraction of background events for each tagging category and background source is given by $f_{i,j}$, while $\hat{b}_{\pm,i,j}$ are parameters used to characterize each source of background by tagging category for mixed and unmixed events. The signal probability $f_{i,\text{sig}}$ is determined from the measured event m_{ES} on the basis of a separate fit to the observed m_{ES} distribution in tagging category i . The sum of signal and background fractions is forced to unity.

The Δt distributions of the background are described with a zero lifetime component and a non-oscillatory component with non-zero lifetime. We fit for separate resolution function parameters for the signal and the background to minimize correlations. The likelihood fit involves a total of 44 parameters, including Δm_d , the average mistag fraction and the difference between B^0 and \bar{B}^0 mistags for each tagging category (8), parameters for the signal Δt resolution (16), and parameters for background time dependence (5), Δt resolution (6), and effective dilutions (8). The value of Δm_d was kept hidden throughout the analysis until all analysis details and the systematic errors were finalized, to eliminate possible experimenter's bias.

The results from the likelihood fit to the tagged B^0 sample are summarized in Table II. The probability to obtain a likelihood smaller than that observed is 44%, evaluated with a parameterized Monte Carlo technique. The value of Δm_d given by the fit, prior to final corrections, is $\Delta m_{d,\text{fit}} = 0.525 \pm 0.016 \text{ ps}^{-1}$. One method for displaying the result of the full likelihood fit is to use the

TABLE II: Results for Δm_d and a subset of the parameters obtained from the likelihood fit to the Δt distributions. Δm_d includes small corrections described in the text.

Parameter	Fit Value	Parameter	Fit Value
Δm_d	0.516 ± 0.016		
w (Lepton)	0.079 ± 0.014	w (NT1)	0.219 ± 0.022
w (Kaon)	0.166 ± 0.012	w (NT2)	0.344 ± 0.020
S_1 (Run1)	1.37 ± 0.09	S_1 (Run2)	1.19 ± 0.11
f_2 (Run1)	0.014 ± 0.010	f_2 (Run2)	0.015 ± 0.010
f_3 (Run1)	0.008 ± 0.004	f_3 (Run2)	0.000 ± 0.014

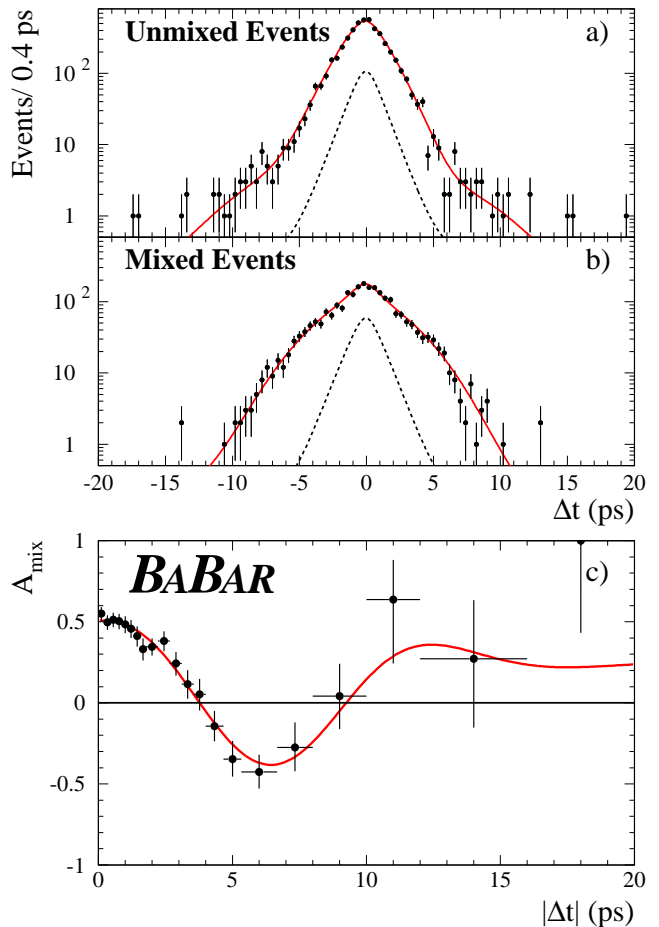


FIG. 2: Distributions of Δt in data for the selected a) unmixed and b) mixed events ($m_{\text{ES}}(B_{\text{rec}}) > 5.27 \text{ GeV}/c^2$), with projections of the likelihood fit (solid) and the contribution of the background (dashed) overlaid. The time-dependent mixing asymmetry $\mathcal{A}_{\text{mix}}(|\Delta t|)$ is shown in c).

observed mixing asymmetry,

$$\mathcal{A}_{\text{mix}}(\Delta t) = \frac{N_{\text{unmixed}}(\Delta t) - N_{\text{mixed}}(\Delta t)}{N_{\text{unmixed}}(\Delta t) + N_{\text{mixed}}(\Delta t)}.$$

If the flavor tagging and Δt determination were perfect, the asymmetry as a function of Δt would be a cosine with unit amplitude. The amplitude is diluted by the mistag

probability and the experimental resolution for Δt . The observed Δt distributions of both the mixed and unmixed events, and their asymmetry \mathcal{A}_{mix} are shown along with projections of the likelihood fit result in Fig. 2.

Since the parameters of the Δt resolution for both signal and backgrounds are free parameters in the fit, their contribution to the uncertainty on Δm_d is included as part of the statistical error. Remaining systematic errors arise from the choice of the signal Δt resolution description, its capability to handle outliers and various worst-case SVT misalignment scenarios ($\pm 0.005 \text{ ps}^{-1}$), and by approximations and uncertainties in the Δz to Δt conversion due to the knowledge of the absolute z scale of the *BABAR* detector and PEP-II boost (less than $\pm 0.002 \text{ ps}^{-1}$). Systematic errors due to background include the choice of its Δt distribution and resolution description ($\pm 0.002 \text{ ps}^{-1}$), variation of the sum of background fractions from the separate m_{ES} fits, and the uncertainty on the magnitude of the small B^+ component of the signal ($\pm 0.002 \text{ ps}^{-1}$). A correction of -0.002 ps^{-1} , derived from data, is made to account for the small variation of the background composition as a function of m_{ES} , which affects the background Δt distribution. The statistical error ($\pm 0.002 \text{ ps}^{-1}$) on this extrapolation from the sideband to the signal region is included as a systematic uncertainty. An additional correction of -0.007 ps^{-1} is applied for a bias observed in fully simulated Monte Carlo events. The bias is mainly due to correlations between the mistag rate and the Δt resolution that are not explicitly incorporated into the likelihood function. The systematic error assigned to this correction includes contributions from the statistical precision of the Monte Carlo study ($\pm 0.003 \text{ ps}^{-1}$), model variations due to uncertain branching fractions and lifetimes of the tag-side D mesons and the assumed fraction of wrong-sign kaons produced in B decays ($\pm 0.001 \text{ ps}^{-1}$), and variation of the requirement on the maximum allowed value of $\sigma_{\Delta t}$ ($\pm 0.003 \text{ ps}^{-1}$). Finally, the variation of the fixed B^0 lifetime within the known errors [4] leads to a systematic uncertainty of $\pm 0.006 \text{ ps}^{-1}$.

In conclusion, a new technique involving the time-difference distribution of a tagged sample of fully-reconstructed neutral B decays has been used to determine the B^0 - \bar{B}^0 mixing frequency Δm_d to be

$$\Delta m_d = 0.516 \pm 0.016(stat) \pm 0.010(syst) \text{ ps}^{-1}.$$

This is one of the single most precise measurements available. Moreover, the error on Δm_d is still dominated by the size of the reconstructed B^0 sample, leaving substantial room for further improvement as more data are accumulated. The result is consistent with the current world average [4] and a recent *BABAR* measurement with a dilepton sample [10]. The analysis shares the same flavor-eigenstate sample as used for the determination of $\sin 2\beta$, thereby providing an essential validation for the reported $\sin 2\beta$ result [5].

We are grateful for the excellent luminosity and machine conditions provided by our PEP-II colleagues. The collaborating institutions wish to thank SLAC for its support and kind hospitality. This work is supported by DOE and NSF (USA), NSERC (Canada), IHEP (China), CEA and CNRS-IN2P3 (France), BMBF (Germany), INFN (Italy), NFR (Norway), MIST (Russia), and PPARC (United Kingdom). Individuals have received support from the Swiss NSF, A. P. Sloan Foundation, Research Corporation, and Alexander von Humboldt Foundation.

* Also with Università di Perugia, Perugia, Italy

† Also with Università della Basilicata, Potenza, Italy

- [1] The symbol B^0 refers to the B_d meson; charge conjugate modes are implied throughout this paper.
- [2] N. Cabibbo, Phys. Rev. Lett. **10**, 531 (1963); M. Kobayashi and T. Maskawa, Prog. Theor. Phys. **49**, 652 (1973).
- [3] UA1 Collaboration, C. Albajar *et al.*, Phys. Lett. **B186**, 247 (1987); ARGUS Collaboration, H. Albrecht *et al.*, Phys. Lett. **B192**, 245 (1987).
- [4] D.E. Groom *et al.*, Eur. Phys. Jour. C **15**, 1 (2000).
- [5] *BABAR* Collaboration, B. Aubert *et al.*, Phys. Rev. Lett. **87**, 151802 (2001).
- [6] *BABAR* Collaboration, B. Aubert *et al.*, *BABAR*-PUB-01/03, to be submitted to Phys. Rev. **D**.
- [7] *BABAR* Collaboration, B. Aubert *et al.*, *BABAR*-PUB-01/08, hep-ex/0105044, to appear in Nucl. Instr. and Methods .
- [8] *BABAR* Collaboration, B. Aubert *et al.*, Phys. Rev. Lett. **87**, 201803 (2001).
- [9] ARGUS Collaboration, H. Albrecht *et al.*, Phys. Lett. **B241**, 278 (1990).
- [10] *BABAR* Collaboration, B. Aubert *et al.*, *BABAR*-PUB-01/22, in preparation.